Inorganic Chemistry

Article

pubs.acs.org/IC

Design and Synthesis of a Noninnocent Multitopic Catechol and Pyridine Mixed Ligand: Nanoscale Polymers and Valence Tautomerism

Mireia Guardingo,[†,‡] Felix Busqué,[§] Fernando Novio,*[,†,‡] and Daniel Ruiz-Molina[†,‡]

[†]ICN2-Institut Català de Nanociència i Nanotecnologia, ICN2 Building, Campus UAB, 08193-Bellaterra, Spain

[‡]CSIC-Consejo Superior de Investigaciones Científicas, ICN2 Building, Campus UAB 08193-Bellaterra, Spain

[§]Chemistry Department, Universitat Autònoma de Barcelona, Campus UAB, 08193-Bellaterra, Spain

Supporting Information

ABSTRACT: The design and synthesis of a new redox-active ligand combining catechol and pyridine units have allowed the achievement of cobalt-based nanoscale coordination polymer particles in a single-step exhibiting a switchable valence tautomeric behavior and thermal hysteresis. The combination of polymerizing capabilities with redox-active responses in a unique ligand leads to the formation of nanoparticles exhibiting a gradual valence tautomeric interconversion in the 35−370 K temperature range. Using one single ligand to obtain these nanoparticles facilitates possible nanostructure formation methodologies.

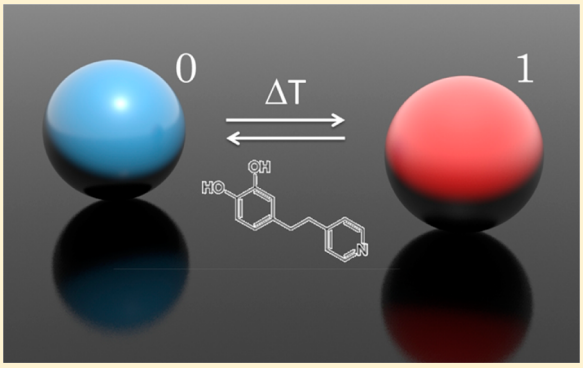

1. INTRODUCTION

Some transition metal complexes bearing redox-active ligands can interconvert between two electronically labile states with different net magnetic moments and optical properties.[1] Both isomers can exist in solution as well as in the solid state and interconvert reversibly by an intramolecular one-electron transfer between the metal ion and the redox-active ligand in response to different external perturbations, such as temperature,[2] pressure,[3] irradiation,[4] and more recently pH.[5] Complexes of this family, termed as valence tautomers (VTs), have been proposed as potential building blocks to obtain molecular switching devices, where the ultimate goal is to manipulate information at the molecular level, build sensors, or display devices.[6]

Most of the VT complexes thus far reported are monomeric[7] and dimeric[8] cobalt complexes containing quinone or quinone-type ligands. They are "noninnocent" electroactive ligands that may interconvert between the semiquinone SQ^{-} and catecholate Cat^{2-} forms in response to an external stimulus (e.g., temperature). However, the potential application of these systems has been limited by the lack of thermal hysteresis, a necessary prerequisite for having memory effects. Indeed, even though hysteresis in a few monomeric[9] and dimeric[10] VT complexes has been reported and associated with their supramolecular packing,[11] crystal engineering did not provide the basic tools for the proper design of molecular systems with hysteresis. To overcome this limitation, some authors focused their efforts toward the design of VT polymers where the constitutive building blocks are mutually interacting through covalent bonds. The schematic representation of the different approaches so far followed for obtaining VT polymers is shown in Figure 1. Within the framework of the first approach (see Figure 1a), one-dimensional[12] and two-dimensional coordination polymers[13] containing cobalt-*o*-quinone complex units are linked by multitopic pyridyl or pyrazol ligands. While the catechol ligand ensures the switchable behavior through the thermally induced intramolecular electron transfer with the cobalt ion, the nonactive multitopic bridging ligand acts as a polymerizing agent, being crucial in the formation of the polymeric structures. Pierpont et al. followed this approach to establish the photomechanical polymer $[Co(pyz)(3,6\text{-}DBQ)_2]_n$.[14] This coordination polymer exhibited a temperature-induced tautomeric interconversion in the solid state and a parallel mechanical process associated with variations on the metal−catechol bond lengths. More recently, three novel polymeric complexes with different bidentate-bridging pyridine ligands were synthesized and their VT behaviors studied.[15] Similarly, a series of 1-D polymer structures ranging from amorphous spherical nanoparticles to crystals with several different morphologies[16] have also been systematically synthesized by controlling experimental parameters such as temperature, reagent concentration, or solvent nature. The experimental results indicated that the degree of crystallinity and the crystalline phase critically determine the VT process, independent of the morphology and/or dimensions of the

Received: March 18, 2015
Published: July 2, 2015

DOI: 10.1021/acs.inorgchem.5b00598
Inorg. Chem. 2015, 54, 6776−6781

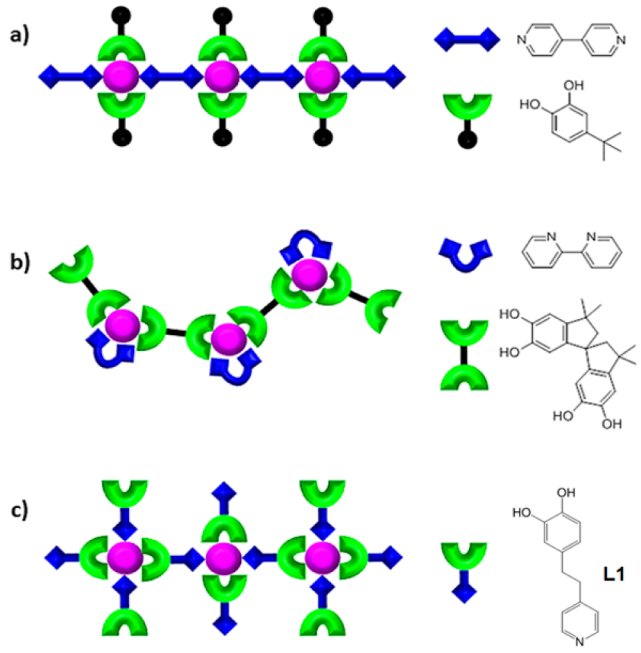

Figure 1. Schematic representation of the different approaches followed so far for the formation of VT coordination polymers: (a) combination of catechol ligands with pyridyl/pyrazol ligands; (b) bis-bidentate catechol and bypiridine counterligands; (c) catechol and pyridine moieties present in the same ligand. Cobalt metal ion is represented by a pink sphere.

crystals. It is worth mentioning that relevant hysteresis effects were not reported in any of the previous examples.

The second approach (see Figure 1b) consists of the use of a bis-bidentate catechol-based ligand as a polymerizing agent and the use of an innocent counter ligand to complete the coordination sphere. The last one is required to achieve the proper balance between the frontier orbitals of the catechol and the metal ion involved in the electron transfer. Following this approach, Schultz and Dei et al. have reported VT coordination polymers[17] and the required cooperative properties that lead to thermal hysteresis. Small hysteresis width (between 5 and 13 K) was found even though the transition could be classified as gradual,[18] which was associated with the existence of cooperativity between the cobalt centers.[19]

Herein we have envisioned a third approach for obtaining coordination polymers with VT based on the use of a sole multitopic ligand that associates both polymerizing capabilities with redox-active responses (see Figure 1c). For this we have designed the new ligand **L1** combining a catechol and a pyridine unit within a single element. A related pyridine derivative catechol ligand designed to behave as a fluorescent chemosensor for wide-range pH detection has already been described, but no examples of coordination complexes were reported due to the high steric hindrance of the ligand.[20] In this case, reaction of the single ligand **L1** with a cobalt salt and its posterior fast precipitation process was successful and afforded the formation of nanoscale coordination polymer particles (**Co-CPPs**). Moreover, the new polymer has been found to exhibit VT and hysteresis effects. Therefore, **L1** not only combines both redox-active and polymerizing capabilities but also allows for the proper balance of localized metal and quinone orbital energies required for the intramolecular electron transfer in VT.

2. EXPERIMENTAL SECTION

Commercially available reagents were used as received. The solvents were dried by distillation over the appropriate drying agents. All reactions were performed avoiding moisture by standard procedures and under nitrogen atmosphere and monitored by analytical thin-layer chromatography (TLC) using silica gel 60 F254 precoated aluminum plates (0.25 mm thickness). Flash column chromatography was performed using silica gel 60 Å, particle size 35−70 μm (230−400 mesh). Final ligand **L1** as well as all the synthetic intermediates involved is pure within the sensibilities of their ^{1}H and ^{13}C NMR spectra.

2.1. Synthesis of Ligand Catechol-Pyridine (L1). Ligand **L1** was obtained following a three-step synthetic methodology shown in Scheme 1 and described below.

Scheme 1. Synthesis of Ligand L1

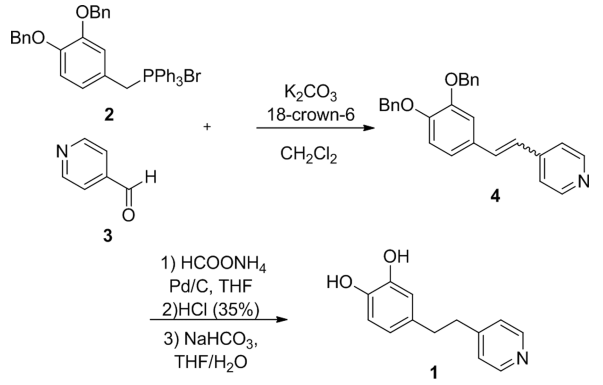

*2.1.1. Synthesis of Z- and E-4-(2-(Pyridin-4-yl)ethenyl)benzene-1,2-dibenzyloxy (**3**).* To a suspension of K_2CO_3 (0.522 g, 3.77 mmol) in dry CH_2Cl_2 (4 mL) was added a small amount of 18-crown-6-ether and **1** (0.527 g, 0.816 mmol) under nitrogen atmosphere. To the resulting mixture a solution of aldehyde **2** (70, 0.652 mmol) in dry CH_2Cl^2 (2 mL) was added, and the mixture was refluxed under nitrogen for 24 h. After that time, the solvent was evaporated, and the crude was purified by flash column chromatography (hexane/EtOAc 80:20) to provide the separation of the 1:1 of *Z*- and *E*-(**3**) fractions (219 mg, 0.557 mmol, 68% yield) as a colorless oil (*Z*-isomer) and white solid (*E*-isomer) after solvent evaporation.

*Characterization of Z-(**3**).* ^{1}H NMR (400 MHz, $CDCl_3$): δ 8.55 (s, 2H: H-11), 7.50−7.29 (m, 12H), 7.19 (d, J = 17.1 Hz, 1H), 7.16 (s, 1H), 7.07 (dd, J = 8.3, 1.9 Hz, 1H), 6.94 (d, J = 8.3 Hz, 1H), 6.81 (d, J = 16.2 Hz, 1H), 5.22 (s, 2H), 5.20 (s, 2H). ^{13}C NMR (100.6 MHz, $CDCl_3$): δ 150.2, 149.9, 149.2, 145.0, 137.2, 137.1, 133.0, 129.9, 128.7, 128.7, 128.1, 128.0, 127.5, 127.4, 124.4, 121.5, 120.8, 114.9, 113.4, 71.6, 71.3.

*Characterization of E-(**3**).* ^{1}H NMR (400 MHz, $CDCl_3$): δ 8.40 (d, J = 4.2 Hz, 2H), 7.44−7.16 (m, 10H), 7.06 (d, J = 5.6 Hz, 2H), 6.76 (m, 2H), 6.70 (dd, J = 8.3, 1.8 Hz, 1H), 6.58 (d, J = 12.2 Hz, 1H), 6.32 (d, J = 12.2 Hz, 1H), 5.09 (s, 2H), 4.88 (s, 2H); ^{13}C NMR (100.6 MHz, $CDCl_3$): 149.8, 148.8, 148.6, 145.5, 137.1, 137.0, 133.6, 129.4, 128.5, 127.9, 127.8, 127.3, 127.1, 126.3, 123.6, 122.6, 115.3, 114.6, 71.2, 71.1.

IR-ATR: υ (cm^{-1}) = 3065, 3027, 2970, 2920, 2856, 1590, 1511, 1267, 1229, 967, 810, 731, 693. HRMS (ESI+) m/z: calcd for $C_{27}H_{23}NO_2$, 394, 1802 $[M + H]^+$; found 394, 1807. Mp 126−130 °C (EtOAc).

*2.1.2. Synthesis of 4-(2-(Pyridinium-4-yl)ethyl)benzene-1,2-diol Chloride (**4**).* A 1:1 mixture of (*Z*)-3 and (*E*)-**3** (439 mg, 1.11 mmol) was dissolved in 10 mL of THF. Then, ammonium formate (391 mg, 6.2 mmol) and Pd/C (10%, 111 mg) were added to the mixture, and it was refluxed for 4 h. The suspension was then filtered over a Celite pad, and a few drops of HCl (35%) were added, resulting in the precipitation of compound **4** as a white solid that was filtrated and rinsed with THF (213 mg, 0.848 mmol, 82% yield). ^{1}H NMR (400

DOI: 10.1021/acs.inorgchem.5b00598
Inorg. Chem. 2015, 54, 6776−6781

MHz, DMSO): δ 8.79 (d, J = 6.6 Hz, 2H), 7.88 (d, J = 6.5 Hz, 2H), 6.63 (d, J = 8.0 Hz, 1H), 6.59 (d, J = 2.0 Hz, 1H), 6.43 (dd, J = 8.0, 2.0 Hz, 1H), 3.11 (t, J = 7.7 Hz, 2H), 2.81 (t, J = 7.7 Hz, 2H). ^{13}C NMR (100.6 MHz, DMSO): δ 162.34 (C-9), 145.1, 143.6, 141.0, 130.6, 127.0, 119.0, 115.9, 115.5, 36.9, 34.4. IR-ATR: υ (cm^{-1}) = 3336, 3197, 2690, 1633, 1610, 1528, 1503, 1202, 811. HRMS (ESI+) m/z: calcd for $C_{13}H_{14}NO_2$, 216, 1019 $[M + H]^+$; found 216, 1028. Mp 176−180 °C (THF).

*2.1.3. Synthesis of 4-(2-(Pyridin-4-yl)ethyl)benzene-1,2-diol (**L1**).* To a suspension of compound **4** (20.4 mg, 0.081 mmol) in THF was added $NaHCO_3$ (9.1 mg, 0.108 mmol) and a few drops of water, and the mixture was stirred at room temperature under nitrogen for 10 min. Then the solvent was evaporated and compound **L1** was obtained as a pale orange solid (17 mg, 85% yield) ^{1}H NMR (400 MHz, MeOD): δ 8.35 (d, J = 5.7 Hz, 2H), 7.20 (d, J = 6.1 Hz, 2H), 6.65 (d, J = 8.0 Hz, 1H), 6.58 (d, J = 2.0 Hz, 1H), 6.45 (dd, J = 8.0, 2.0 Hz, 1H), 2.90 (t, J = 7.4 Hz, 2H), 2.78 (t, J = 7.7 Hz, 2H); ^{13}C NMR (100.6 MHz, MeOD): δ 153.9, 149.6, 146.1, 144.6, 133.6, 125.8, 120.8, 116.6, 116.3, 38.4, 36.9; IR-ATR: υ (cm^{-1}) = 3028, 2923, 2853, 1602, 1527, 1486, 1250, 805, 643, 586, 503; Anal. Calcd (%) for $C_{13}H_{13}NO_2$: C, 72.54; H, 6.09; N, 6.51. Found: C, 72.68; H, 6.26; N, 6.37; HRMS (ESI+) m/z: calcd for $C_{13}H_{14}NO_2$, 216, 1019 $[M + H]^+$; found 216, 1025. Mp 170−174 °C.

2.2. Synthesis of Cobalt-Based Coordination Polymer Particles (Co-CPPs). An aqueous solution (4 mL) of Co-$(CH_3COO)_2{\cdot}4H_2O$ (121.4 mg, 0.50 mmol) was added dropwise to a solution of ligand **L1** (216.1 mg, 1 mmol) in EtOH (20 mL). A black precipitate formed immediately. After 30 min of reaction time the precipitate was centrifuged and washed several times with water and EtOH, and dried under vacuum. The resulting solid product obtained in 70% yield. SEM analysis showed the spherical morphology (mean size: 109 ± 12 nm), and XRD measurements indicate the amorphous nature of the particles. IR-ATR: υ (cm^{-1}) = 3350, 2957, 2924, 2856, 1597, 1482, 1277, 1222, 1184, 1112, 1068, 821, 620, 533. Anal. Calcd for $C_{26}H_{22}O_4CoN_2$: C,64.34; H, 4.57; N, 5.77. Found: C, 64.79; H, 4.66; N, 5.83.

2.3. Physicochemical Characterization. H NMR spectra were recorded on Bruker DPX250 (250 MHz), DPX360 (360 MHz) and ARX400 (400 MHz) spectrometers. Proton chemical shifts are reported in ppm (δ) ($CDCl_3$, δ 7.26 or CD_3OD, δ 3.31). ^{13}C NMR spectra were recorded on Bruker DPX360 (90 MHz) spectrometers with complete proton decoupling. Carbon chemical shifts are reported in ppm (δ) ($CDCl_3$, δ 77.0 or CD_3OD, δ 49.0). The IR-ATR spectra have been recorded using a Tensor 27 (Bruker) spectrophotometer. The melting points (Mp's) have been determined using a Reichert kofler block and have not been corrected. Size distribution of the nanoparticles was measured by DLS, using the Zetasizer Nano 3600 instrument (Malvern Instruments, U.K.). Note that the diameter measured by DLS is the hydrodynamic diameter. All samples were diluted to obtain an adequate nanoparticle concentration. The data reported are mean values for each sample, which were measured in quadruplicate. The UV−vis spectra were recorded using a Cary 4000 spectrophotometer and a 1 cm path length quartz cuvette. The baseline was corrected using a blank sample of pure solvent. Powder XRD spectra were recorded at room temperature on a high-resolution texture diffractometer (PANalytical X'Pert PRO MRD) equipped with a Co Kα radiation source (λ = 1.7903 Å) and operated in reflection mode. The solid samples were placed in an amorphous silicon oxide flat plate and measured directly. SEM images were performed on a scanning electron microscope (FEI Quanta 650 FEG) at acceleration voltages between 2 and 5 kV. Aluminum was used as support. The samples were prepared by drop casting of the corresponding dispersion on aluminum tape followed by evaporation of the solvent under room conditions. Before analysis, the samples were metalized with a thin layer of gold by using a sputter coater (Emitech K550). Energy-dispersive X-ray spectroscopy (EDX) analysis were performed using a Quanta 650 FEG microscope equipped with an Inca 250 SSD XMax20 detector Peltier cooled with 20 mm^2 active area and 129 eV resolution. Variable-temperature magnetic characterization was done in a Quantum Design MPMS XL SQUID on the 35−370 K temperature range operating at a magnetic field strength of 0.1 T. Raman spectra were acquired at different temperatures using a Dilor triplemate spectrograph (1800 1/mm grating, 100 μm entrance slit, 1 cm^{-1} spectral resolution) coupled to a Princeton Instruments CCD detector. The 647.1 nm line of a Kr^+ laser (Coherent RadiationInnova) was used as an excitation source with laser power output of 10 mW.

3. RESULTS AND DISCUSSION

3.1. Synthesis of Ligand L1 and Polymerization Reaction. Ligand **L1** was obtained following a synthetic strategy already reported in our group (Scheme 1).[21] The first step consists of a Wittig reaction between the previously described phosphorane derivative of compound **1** and 4-pyridinecarboxaldehyde (**2**) to obtain a (1:1) mixture of *Z*- and *E*-4-(2-(pyridin-4-yl)ethenyl)benzene-1,2-dibenzyloxy (**3**) in 68% yield. This mixture of olefins was hydrogenated, using ammonium formate under palladium catalyst, with concomitant deprotection of the hydroxyl groups. Subsequent addition of concentrated HCl led to the precipitation of **4** with 82% overall yield in the three last reactions. Finally, compound **4** was neutralized to obtain the desired ligand **L1** that contains the two functional groups (catechol and pyridine) required. Afterward, nanoscale coordination polymer particles **Co-CPPs** were obtained by mixing an aqueous solution of cobalt acetate with an ethanolic solution containing 2 equiv of **L1** under magnetic stirring. The precipitate formed by in situ polymerization and fast precipitate was collected after 30 min, washed several times with water and EtOH, and dried under vacuum resulting in the formation of spherical particles as previously reported.[22] CPPs exhibit average diameters between 60 and 130 nm (mean size 110 nm), as found by scanning electron microscopy (SEM) (see Figure 2b) and confirmed by dynamic light scattering (DLS) (see Supporting Information Figure S1). Moreover, nanoparticle diameters could be controlled by regulating the stirring rate (see Supporting Information Figure S2) or modifying the synthetic approach. For instance, larger nanoparticles (average diameter between 400 nm and 1 μm) were obtained by slow diffusion of the cobalt aqueous solution into an alcoholic solution of the ligand **L1**, without stirring (see Figure 2a).

3.2. Characterization. X-ray powder diffraction of the different batches obtained showed that the particles are amorphous materials preventing a detailed analysis of the structural connectivity (see Supporting Information Figure S3). However, the infrared spectra of the obtained particles corroborate the coordination of the metal center as revealed by the displacement of the main bands attributed to the C—O stretching of the catecholate mode (1280−1250 cm^{-1} range), those corresponding to the C═C/C—N stretching modes (1530−1400 cm^{-1}), the bands in the 900−750 cm^{-1} range attributed to the C−H bend in the aromatic ring, and those in the 700−500 cm^{-1} region corresponding to Co—O and Co—N vibrations (see Supporting Information Figure S4). Energy-dispersive X-ray spectroscopy (EDX) and elemental analysis also confirmed that this material contains cobalt, carbon, oxygen, and nitrogen in ratios that are consistent with the proposed polymeric structure (see Supporting Information Figure S5). The thermogravimetric analysis (TGA) performed under N_2 atmosphere indicates a good stability up to 175 °C with only a small weight loss around 5% at temperatures higher that 75 °C, tentatively assigned to the removal of entrapped solvent (water or most likely ethanol) within the nanoparticles.

DOI: 10.1021/acs.inorgchem.5b00598
Inorg. Chem. 2015, 54, 6776−6781

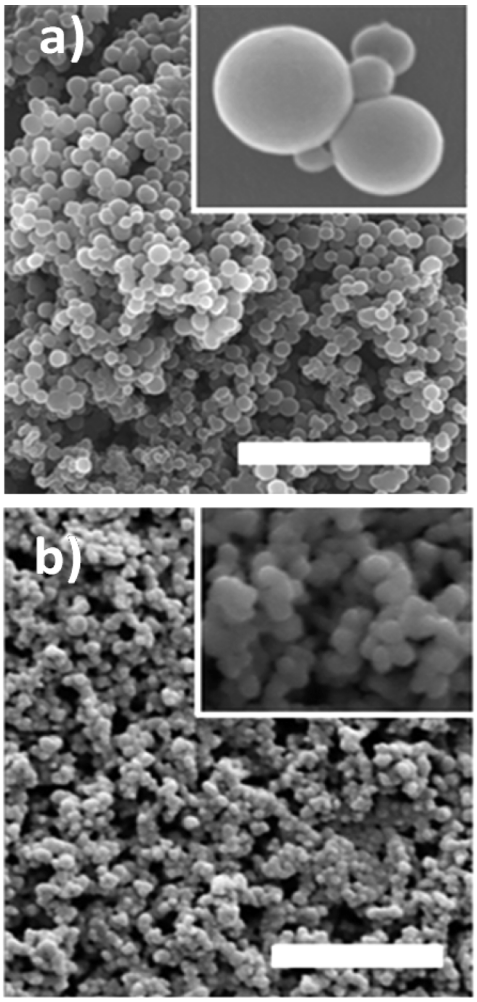

Figure 2. SEM images showing the morphology of **Co-CPPs** obtained by using different experimental procedures: (a) spherical microsize particles obtained by a diffusion process (bar = 10 μm) and (b) nanoparticles obtained under magnetic stirring (bar = 2 μm).

From 175 to 325 °C a gradual weight loss attributed to the loss of **L1** molecules is observed, whereupon a definitive and drastic thermal decomposition of the material takes place up to 400 °C (see Supporting Information Figure S6).

3.3. Valence Tautomerism. Figure 3 shows the temperature dependent magnetic susceptibility of **Co-CPPs** in the 35−370 K temperature range. At the highest temperature of 370 K the resulting experimental μ_{eff} value of 4.4 μ_B is close to the theoretical values expected for a $S = {}^3/_2 + 2 \times {}^1/_2$ species with an unquenched orbital contribution (4.6 μ_B). Upon cooling, the μ_{eff} value monotonically decreases down to 2.6 μ_B at 35 K. A fit to a line through the lowest temperature points finally determines a *y*-intercept around 1.90 μ_B, close to the 1.73 μ_B theoretical value for a $S = {}^1/_2$ system Co(III) ground state. On the other side, the gradual interconversion, which is commonly observed in noncrystalline phases and tautomeric coordination polymers,[23] could be tentatively attributed to the interconversion from the hs-Co(II) isomer to the ls-Co(III) isomer together with spin−orbit coupling effects[24] or the possible presence of an additional structural transition.[25] Moreover, though less probable, since the actual magnetic structure is not at all known, the possibility of a ferromagnetic (Hund's) ground state could not be discarded at this stage.

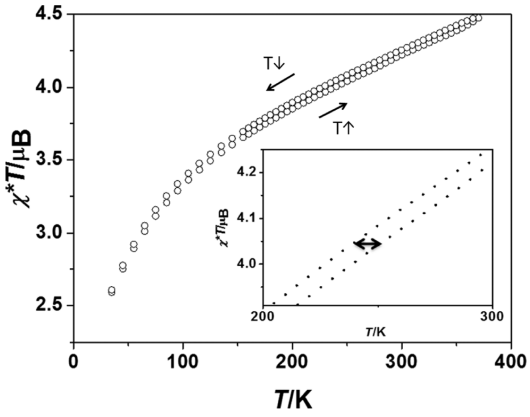

Figure 3. Variable-temperature magnetization measurements in the 35−370 K temperature range. Inset: Difference in the measured μ_{eff} between heating (bottom line) and cooling (upper line) processes. The arrow in the inset figure shows the maximum width of thermal hysteresis, ca. 12 at 250 K.

UV−vis spectroscopy of a dispersion of **Co-CPPs** in toluene at two different temperatures also confirmed the VT interconversion (see Supporting Information Figure S7). In both spectra bands at 590 nm, characteristic of ls-Co(III) isomer, and 740 nm associated with the hs-Co(II) isomer were observed.[14,16,26] As the temperature is increased, the intensity of the band at 590 nm decreases while the band at 740 nm becomes more intense, in agreement with the existence of VT equilibrium. Moreover, this process is fully reversible over different cycles. In addition, studies at different temperatures were performed using Raman spectroscopy to check changes associated with the VT process between 80 and 373 K (see Supporting Information Figure S8). Thus, an increasing intensity of the signals assigned to intraligand catecholate vibrations, either C−C stretching, υ(C−C), between 1300 and 1590 cm^{-1}, or C−H deformation, δ(C−H), at 1190 cm^{-1}, were observed as the temperature was decreased.[27] This fact is in agreement with the increasing ls-Co(III) isomer population at low temperatures and provide further evidence for the valence tautomerism.

The existence of VT on the **Co-CPPs** nanoparticles is not only important for their implications in future molecular electronic devices but also for the structural characterization of the material. Indeed, even though the amorphous nature of **Co-CPPs** nanoparticles precludes any accurate structural characterization by classical diffraction techniques, the occurrence of VT corroborates the expected [Co(nitrogen)(quinone)] composition required to ensure a proper energy balance between the antibonding orbital (e_g orbital) of the metal ion and the frontier orbitals of catechol ligands for the intramolecular electron transfer to take place.

Another important feature of these nanoparticles is the observation of small hysteresis effects (see inset in Figure 3); when the nanoparticles are subjected to thermal cycling over the whole temperature range studied, the curves associated with the increase and decrease of the temperature differ by almost 12 K. Such hysteresis is reproducible over different cycles discarding any influence of small composition variations. Moreover, no dependence with the sweeping rate was found discarding a spin frustration mechanism as its origin.

DOI: 10.1021/acs.inorgchem.5b00598
Inorg. Chem. 2015, 54, 6776−6781

4. CONCLUSIONS

In summary, we have designed and synthesized the new bifunctional ligand **L1** that combines both polymerizing capabilities with redox-active responses by covalently linking catechol and pyridine units. The coordination of **L1** upon reaction with cobalt ions and its subsequent polymerization and precipitation leads to the formation of nanoparticles a few hundred nanometers in width exhibiting a gradual VT interconversion in the 35−370 K temperature range. An important feature of these nanoparticles is the observation of a small hysteresis effect that can be related to the cooperative effect between valence tautomeric units induced by the catechol-pyridyl ligand. The midpoints of the cooling and heating curves differ by almost 12 K. Such hysteresis is similar to the one obtained in a previous work by using bis-catecholate ligands (approach 2 of Figure 1)[17,18] whereas no hysteresis has been found for coordination polymers containing cobalt-*o*-quinone complex units linked by multitopic pyridyl or pyrazol ligands (approach 1 of Figure 1). This fact suggests the need for the catechol to be involved in the polymerization process to induce the hysteresis effect. Using one single ligand to obtain these nanoparticles could enable possible nanostructuration methodologies

■ ASSOCIATED CONTENT

Ⓢ Supporting Information

Dynamic light scattering, calorimetric studies, powder X-ray diffraction, energy-dispersive X-ray spectroscopy, ATR-IR and UV−vis spectroscopy, and scanning electron microscopy images. The Supporting Information is available free of charge on the ACS Publications website at DOI: 10.1021/acs.inorgchem.5b00598.

■ AUTHOR INFORMATION

Corresponding Author

*E-mail: fnovio@cin2.es.

Author Contributions

The manuscript was written through contributions of all authors. All authors have given approval to the final version of the manuscript. In addition, M.G. has synthesized ligand **L1**. F.N. has synthesized and characterized the nanoparticles. F.N., D.R.-M., and F.B. supervised the project and coordinated the preparation of the manuscript.

Funding

Ministerio de Ciencia e Innovación (MICINN) through projects MAT2012-38318-C03-02, MAT2012-38319-C02-01, CTQ2013-41161-R, and CTQ2010-15380, and FEDER funds. The authors declare no competing financial interests.

Notes

The authors declare no competing financial interest.

■ ACKNOWLEDGMENTS

This work was supported ICN2 acknowledges support from the Severo Ochoa Program (MINECO, Grant SEV-2013-0295). F.N. thanks the Ministerio de Ciencia e Innovación (MICINN) for a JdC fellowship. M.G. thanks the Consejo Superioir de Investigaciones Científicas (CSIC) for a JAE fellowship. The authors also thank ECOSTBio Cost Action and Dr. G. Molnar and Prof. A. Bousseksou for Raman measurements and very helpful discussions.

■ REFERENCES

(1) (a) Evangelio, E.; Ruiz-Molina, D. *Eur. J. Inorg. Chem.* **2005**, 2957−2971. (b) Gütlich, P.; Dei, A. *Angew. Chem., Int. Ed. Engl.* **1997**, *36*, 2734−2736.

(2) Tezgerevska, T.; Alley, K. G.; Boskovic, C. *Coord. Chem. Rev.* **2014**, *268*, 23−40.

(3) Roux, C.; Adams, D. M.; Itié, J. P.; Polian, A.; Hendrickson, D. N.; Verdaguer, M. *Inorg. Chem.* **1996**, *35*, 2846−2852.

(4) Sato, O.; Cui, A.; Matsuda, R.; Tao, J.; Hayami, S. *Acc. Chem. Res.* **2007**, *40*, 361−369.

(5) Nador, F.; Novio, F.; Ruiz-Molina, D. *Chem. Commun.* **2014**, *50*, 14570−14572.

(6) (a) González-Monje, P.; Novio, F.; Ruiz-Molina, D. *Chem.—Eur. J.* **2015**, *21*, 1−7. (b) Dei, A.; Gatteschi, D. *Angew. Chem., Int. Ed.* **2011**, *50*, 11852−11858. (c) Sato, O.; Cui, A.; Matsuda, R.; Tao, J.; Hayami, S. *Acc. Chem. Res.* **2007**, *40*, 361−369. (d) Hendrickson, D. N.; Pierpont, C. G. *Top. Curr. Chem.* **2004**, *234*, 63−95. (e) Gütlich, P.; Garcia, Y.; Goodwin, H. A. *Chem. Soc. Rev.* **2000**, *29*, 419−427.

(7) (a) Mulyama, Y.; Poneti, G.; Moubaraki, B.; Murray, K. S.; Abrahams, B. F.; Sorace, L.; Boskovic, C. *Dalton Trans.* **2010**, *39*, 4757−4767. (b) Adams, D. M.; Dei, A.; Rheingold, A. L.; Hendrickson, D. N. *J. Am. Chem. Soc.* **1993**, *115*, 8221−8229. (c) Buchanan, R. M.; Pierpont, C. G. *J. Am. Chem. Soc.* **1980**, *102*, 4951−4957.

(8) (a) Poneti, G.; Mannini, M.; Cortigiani, B.; Poggini, L.; Sorace, L.; Otero, E.; Sainctavit, Ph.; Sessoli, R.; Dei, A. *Inorg. Chem.* **2013**, *52*, 11798−11805. (b) Alley, K. G.; Poneti, G.; Robinson, P. S. D.; Nafady, A.; Moubaraki, B.; Aitken, J. B.; Drew, S. C.; Ritchie, Ch.; Abrahams, B. F.; Hocking, R. K.; Murray, K. S.; Bond, A. M.; Harris, H. H.; Sorace, L.; Boskovic, C. *J. Am. Chem. Soc.* **2013**, *135*, 8304−8323. (c) Bin-Salamon, S.; Brewer, S. H.; Depperman, E. C.; Franzen, S.; Kampf, J. W.; Kirk, M. L.; Kumar, R. K.; Lappi, S.; Peariso, K.; Preuss, K. E.; Shultz, D. A. *Inorg. Chem.* **2006**, *45*, 4461−4467.

(9) (a) Schmidt, R. D.; Shultz, D. A.; Martin, J. D.; Boyle, P. D. *J. Am. Chem. Soc.* **2010**, *132*, 6261−6273. (b) Pierpont, C. G. *Coord. Chem. Rev.* **2001**, *216−217*, 99−126. (c) Jung, O. K.; Jo, D. H.; Lee, Y.-A; Conklin, B. J.; Pierpont, C. G. *Inorg. Chem.* **1997**, *36*, 19−24.

(10) (a) Yu, F.; Xiang, M.; Wu, Q. G.; He, H.; Cheng, S.-Q.; Cai, X.-y.; Li, A.-h.; Zhang, Y.-m. *Inorg. Chim. Acta* **2015**, *426*, 146−149. (b) Li, B.; Tao, J.; Sun, H.-L.; Sato, O.; Huang, R.-B.; Zheng, L.-S. *Chem. Commun.* **2008**, 2269−2271. (c) Tao, J.; Maruyama, H.; Sato, O. *J. Am. Chem. Soc.* **2006**, *128*, 1790−1791.

(11) Adams, D. M.; Dei, A.; Rheingold, A. L.; Hendrickson, D. N. *J. Am. Chem. Soc.* **1993**, *115*, 8221−8229.

(12) (a) Chen, L. Q.; Wei, R.; Tao, J.; Huang, R.; Zheng, L.-S. *Sci. China Chem.* **2012**, *55*, 1037−1041. (b) Attia, A. S.; Pierpont, C. G. *Inorg. Chem.* **1995**, *34*, 1172−1179. (c) Cheng, W. Q.; Li, G. L.; Zhang, R.; Ni, Z.-H.; Wang, W. F.; Sato, O. *J. Mol. Struct.* **2015**, *1087*, 68.

(13) Li, B.; Chen, L.-Q.; Wei, R.-J.; Tao, J.; Huang, R.-; Zheng, L.-S.; Zheng, Zh. *Inorg. Chem.* **2011**, *50*, 424−426.

(14) Jung, O.-S.; Pierpont, C. G. *J. Am. Chem. Soc.* **1994**, *116*, 2229−2230.

(15) Chen, X.-Y.; Wei, R.-J.; Zheng, L. S.; Tao, J. *Inorg. Chem.* **2014**, *53*, 13212−13219.

(16) Novio, F.; Campo, J.; Ruiz-Molina, D. *Inorg. Chem.* **2014**, *53*, 8742−8748.

(17) Affronte, M.; Beni, A.; Dei, A.; Sorace, L. *Dalton Trans.* **2007**, *43*, 5253−5259.

(18) Bodnar, S. H.; Caneschi, A.; Dei, A.; Shultz, D. A.; Sorace, L. *Chem. Commun.* **2001**, 2150−2151.

(19) (a) Kiriya, D.; Nakamura, K.; Kitagawa, S.; Chang, H.-Ch. *Chem. Commun.* **2010**, *46*, 3729−3731. (b) Kiriya, D.; Chang, H.-Ch; Nakamura, K.; Tanaka, D.; Yoneda, K.; Kitagawa, S. *Chem. Mater.* **2009**, *21*, 1980−1988. (c) Kiriya, D.; Chang, H.-Ch; Kitagawa, S. *J. Am. Chem. Soc.* **2008**, *130*, 5515−5522.

(20) (a) Evangelio, E.; Hernando, J.; Imaz, I.; Bardají, G. G.; Alibés, R.; Busqué, F.; Ruiz-Molina, D. *Chem.—Eur. J.* **2008**, *14*, 9754−9763.

DOI: 10.1021/acs.inorgchem.5b00598
Inorg. Chem. 2015, 54, 6776−6781

(b) Martínez-Otero, A.; Busqué, F.; Hernando, J.; Ruiz-Molina, D. *Nanoscale* **2010**, *2*, 1781−1788.
(21) Guardingo, M.; Bellido, E.; Miralles-Llumà, R.; Faraudo, J.; Sedó, J.; Tatay, S.; Verdaguer, A.; Busqué, F.; Ruiz-Molina, D. *Small* **2014**, *10*, 1594−1602.
(22) (a) Imaz, I.; Maspoch, D.; Rodríguez-Blanco, Cl.; Pérez-Falcón, J. M.; Campo, J.; Ruiz-Molina, D. *Angew. Chem., Int. Ed.* **2008**, *47*, 1857−1860. (b) Novio, F.; Ruiz-Molina, D. *RSC Adv.* **2014**, *4*, 15293−15296.
(23) (a) Evangelio, E.; Ruiz-Molina, D. *C. R. Chim.* **2008**, *11*, 1137−1154. (b) Evangelio, E.; Rodriguez-Blanco, C.; Coppel, Y.; Hendrickson, D. N.; Sutter, J. P.; Campo, J.; Ruiz-Molina, D. *Solid State Sci.* **2009**, *11*, 793−800.
(24) Lloret, F.; Julve, M.; Cano, J.; Ruiz-García, R.; Pardo, E. *Inorg. Chim. Acta* **2008**, *361*, 3432−3445.
(25) Beni, A.; Dei, A.; Shultz, D. A.; Sorace, L. *Chem. Phys. Lett.* **2006**, *428*, 400−404.
(26) (a) Novio, F.; Evangelio, E.; Vazquez-Mera, N.; Gonzalez-Monje, P.; Bellido, E.; Mendes, S.; Kehagias, N.; Ruiz-Molina, D. *Sci. Rep.* **2013**, *3*, 1708. (b) Katayama, K.; Hirotsu, M.; Kinoshita, I.; Teki, Y. *Dalton Trans.* **2014**, *43*, 13384−13391.
(27) Hartl, F.; Barbaro, P.; Bell, I. M.; Clark, R. J. H.; Snoeck, T. L.; Vlček, A., Jr. *Inorg. Chim. Acta* **1996**, *252*, 157−166.

DOI: 10.1021/acs.inorgchem.5b00598
Inorg. Chem. 2015, 54, 6776−6781